ISSN 1054-660X, Laser Physics

Surface Ablation of Congruent and Mg-Doped Lithium Niobate by Femtosecond Laser[1]

H. Lao, H. Zhu, and X. Chen*

The State Key Laboratory on Fiber Optic Local Area Communication Networks and Advanced Optical Communication Systems, Department of Physics, Shanghai Jiao Tong University, 800 Dongchuan Road, Shanghai, 200240 China

*e-mail: xfchen@sjtu.edu.cn

Received July 11, 2009; in final form, July 27, 2009; published online December 7, 2009

Abstract—Lithium niobate is praised as silicon in nonlinear optics for its wide usage both in fundamental science and applications in optics. But its photorefractive effect hinders it from more extensive application in optics. The deadlock has been broken by doping some metallic elements such as magnesium into the congruent lithium niobate crystal for its high damage resistance. The single-shot and multi-shot surface ablation experiments by femotosecond laser with the wavelength of 800 nm and the duration of 80 fs were conducted in the same condition and the ablation threshold fluence was gained for congruent lithium niobate crystal and 6 mol % Mg-doped lithium niobate crystal. The band gap widening after doping is responsible for the discrepancy of the ablation thresholds between the two samples. The laser threshold fluence dependence of laser-shot number demonstrates the difference of the accumulation effect. The large reduction of trapping cross section for electrons after heavy doping of magnesium is focused more to interpret this distinction.

PACS numbers: 52.38.Mf, 77.84.Dy, 42.62.-b

DOI: 10.1134/S1054660X1001010X

INTRODUCTION

For several decades, lithium niobate (LN), regarded as silicon in nonlinear optics, has been of great interest for both fundamental science and applications in optics because of its excellent acousto-optic, electro-optic, elastic-optic, piezoelectric, pyroelectric, nonlinear optical, and optical waveguiding properties [1–3]. However, one of its eminent properties: photorefractive effect (or light-induced optical damage) is a drawback in many fields of optics such as optical modulation and frequency doubling to a great extent [4]. In 1984, Bryan et al. claimed the damage resistance of LN can be increased by a factor of 100 in case that the crystals are heavily doped with MgO [5]. Since then, efforts have been made to indicate that the unwanted photorefractive damage of LN can be suppressed by doping the material with magnesium [6–8].

Until now, LN is still widely used in lots of aspects in optics, such as the research on quasi-phase-matched technique by periodically poled lithium niobate (PPLN). And, with the development of ultrashort pulse laser characterized by its high peak power, femotosecond laser ablations on different kinds of material, even on the biological tissues such as human teeth as a promisingly innovative therapy to dental hard tissues pathologies [9], have been studied. Moreover, attempts are made to study on the propagation of ultrashort pulse, especially femtosecond laser in PPLN [10, 11]. Meanwhile, trends to substitute LN with Mg:LN make a brilliant figure in some certain regions [12, 13]. Thereby, it is of significance to determine the ablation threshold of these two materials by ultrashort pulse, both in the deeper understanding of ferroelectric crystals anti-damage characteristics and in ultrashort-pulse microfabrication in such crystals.

In this paper, the surface ablation of congruent lithium niobate and Mg-doped lithium niobate under irradiation by single and multi femtosecond laser pulses has been studied, of which the ablation thresholds have been determined. The shot-number dependence on the surface-damage threshold of both two crystals for femtosecond laser pulse illumination is discussed next, thus demonstrating the properties discrepancy of congruent and Mg-doped lithium niobate. The variations of band gap and trapping cross section for electrons after doping are applied to explain the distinction in damage threshold and incubation effect.

EXPERIMENTAL SETUP

The test samples are a Z-cut 20 mm × 10 mm × 1 mm ($X \times Y \times Z$) congruent lithium niobate crystal and a Z-cut 20 mm × 10 mm × 0.5 mm ($X \times Y \times Z$) 6 mol % Mg-doped lithium niobate crystal, in optical polishing on both sides. In our ablation experiment, a regeneralized amplified Ti:sapphire femtosecond laser beam with the wavelength of 800 nm and the duration of 80 fs at 1-kHz repetition rate was employed to be vertically focused on the surface of the samples through an optical lens with a focal length of 70 mm. A Guassian spatial beam profile with a $(1/e^2)$ radius

[1] The article is published in the original.

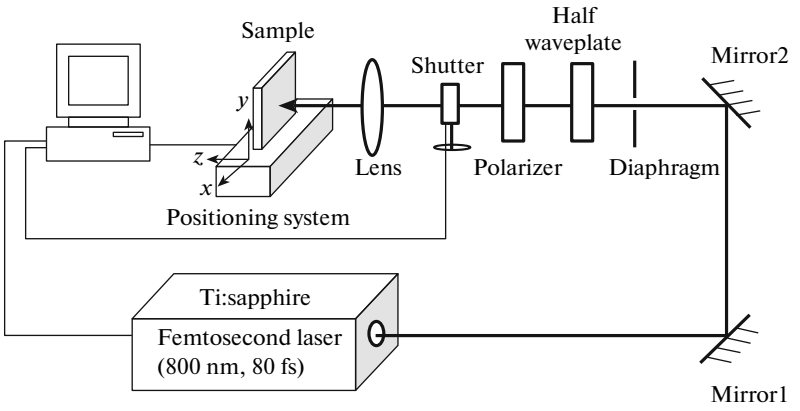

Fig. 1. Experimental setup for femtosecond laser surface ablation of LN and 6 mol % Mg:LN.

~15 μm at the spot was achieved. In front of the optical lens, the pulse energy can be continuously adjusted via a combination of a rotatable half-wave plate followed by a polarizer with another function to ensure that each pulse acted on the samples is in the same polarization. A speed-controllable shutter was utilized to obtain a desired pulse train with certain pulses. The targets were positioned on a stepping-motor-controlled stage in the way that their surfaces (both are X–Y planes) were normal to the incident direction of laser beam. The written repetition of laser was set at 10 Hz. A simplified picture of experimental setup is illustrated in Fig. 1.

We conducted the single-shot and multi-shot surface modifications on the congruent and 6 mol % Mg-doped LN samples in the same day, which makes sure that the experimental conditions remained basically unchanged.

EXPERIMENTAL RESULTS AND DISCUSSIONS

Generally speaking, the laser surface ablation is material specific and intensively depends on laser parameters such as spatial-beam profile, laser fluence, pulse duration, shots number, et al. For our experimentation, the pulse duration and the performance of the laser system were relatively stable for one-day test. Since the incident laser beam has a Gaussian spatial profile with a $1/e^2$-beam radius ω_0, a concise relationship can be derived among the diameter of the ablated area D, the laser ablation-threshold fluence threshold F_{th}, the peak laser fluence F_0 and ω_0, as follows [14, 15].

For a beam with a Gaussian-shape spatial distribution, the laser fluence can be written as

$$F_{laser} = F_0 \exp\left(-\frac{2r^2}{\omega_0^2}\right), \quad (1)$$

where r is the distance from the center point of the beam, and the maximum laser fluence F_0 has a linearly relation with the incident pulse energy E_{pulse}:

$$F_0 = \frac{2E_{pulse}}{\pi\omega_0^2}. \quad (2)$$

The laser ablation threshold is the pulse fluence at $r = D/2$, thereby achieving the simple relationship as:

$$D^2 = 2\omega_0^2 \ln\left(\frac{F_0}{F_{th}}\right). \quad (3)$$

From the above equations, the ablation threshold can be obtained by measuring a series of D under different pulse energies. The measurement work of diameters of the laser-damaged areas was accomplished under a digital optical microscope. Figures 2a and 2b show the typical snapshot pictures of the ablated area of the congruent and Mg-doped samples respectively under single-shot work, which are the results of 400 times amplification. In this case, the pulse energies were both 220 μJ. The shapes of the ablated area are tilted ellipses which are mainly caused by fact that the incident pulse spatial distribution was not ideally Gauss-

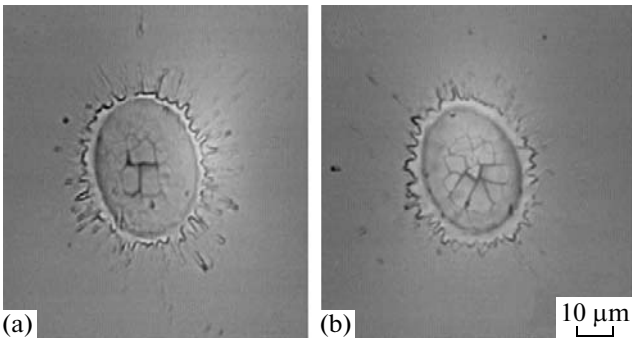

Fig. 2. The micrograph of single-shot ablated spots of (a) LN and (b) 6 mol % Mg-doped LN under the pulse energy at 220 μJ by femtosecond laser.

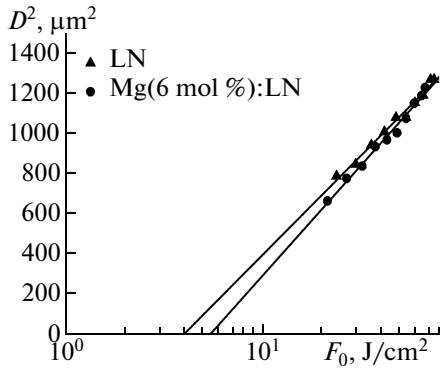

Fig. 3. The relationship between the squared diameters of the ablated areas and laser fluence for single pulse processing of congruent and 6 mol % Mg-doped LN crystals.

ian-profile. From these two micrographs, it is found that the ablated diameter of Mg-doped crystal is imperceptibly tinier than the congruent one, which is due to the distinction of the ablation threshold of them.

Figure 3 reveals the measured fluence dependence of the squared diameters of ablated area for two samples under single shot. In accordance with Eq. (3), the slopes of the fitted lines give the information of the beam radius ($1/e^2$) ω_0 which is 14.6 μm for the congruent sample and 15.4 μm for the doped one. The slight instability of the laser system and the unavoidable errors of measurement are responsible for the tiny disparity in the slopes. Considering the errors is in tolerance range, the data processing employed the different ω_0 for the two materials in the following part. By extrapolate the fitted line to $D^2 = 0$, the thresholds are $F_{th} = 3.92$ J/cm^2 to congruent lithium niobate and $F_{th} = 5.34$ J/cm^2 to 6 mol % Mg-doped lithium niobate, approximately 1.36 times of the congruent one, which indicates the truth that doping Mg will improve the optical anti-damage property of lithium niobate dramatically.

In general, the ablation of the dielectric materials by ultrashort pulse can be depicted by means of three primary progresses. Initially conduction-band electrons must be generated to start the ablation process by the light via strong-field ionization (mainly multiphoton ionization by femtosecond laser irradiation) as described by Keldysh [16]. Then follows the collision process in which multiplication can take place by avalanche ionization. When the conduction-band electron density reach the plasma density, the absorption increases significantly and thereby ablation will occur. During these processes, the band gap is one of the parameter which has a great impact on the ablation threshold [17]. Doping Mg into lithium niobate crystal broadens the band gap [18] and thus higher energies are required for multiphoton and avalanche ionizations, especially for the former one inasmuch as it provides the "seed electrons" for the latter one, which is responsible for the higher ablation threshold fluence of Mg-doped lithium niobate. The results of the multi-shot experiment confirm it again but accumulation effect should be laid more emphasis on in multi-shot condition.

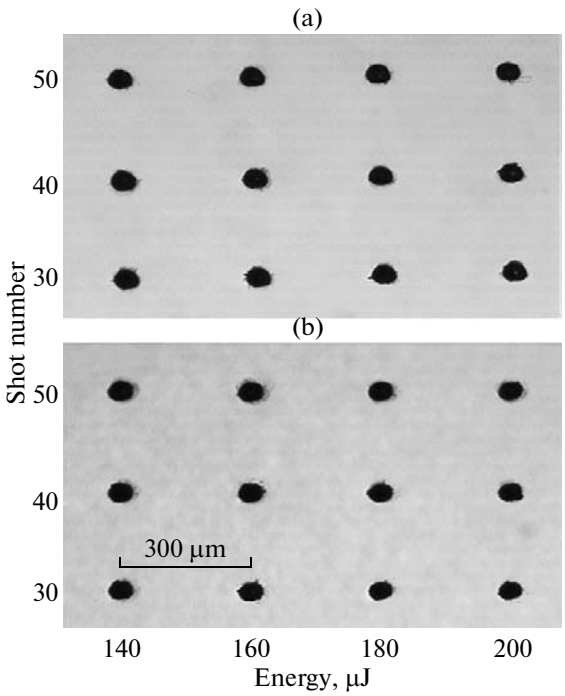

Fig. 4. The micrograph of ablation spot matrixes of the surfaces of (a) LN and (b) 6 mol % Mg-doped LN under multi shots (energy increases from left to right and shot number decreases from top to bottom).

Multi-shot experiments were performed next for further insight into the differentiation between the couple of crystals on multi-shot threshold fluence as well as accumulation effect. The ablation matrix in Fig. 4a was taken under 40 times enlargement and displays variation of the ablated area for congruent sample with varied incident energies and shot number. The

Laser ablation of congruent LN and Mg (6 mol %):LN under multi-shot experiment

Shot number	1	20	30	40	50	60	70	80	90	100	300	500
$F_{th\text{-}LN}$/J cm^{-2}	3.92	1.74	1.44	1.23	1.19	1.14	1.10	1.17	1.20	1.18	1.21	1.17
$F_{th\text{-}Mg:LN}$/J cm^{-2}	5.34	2.88	2.49	2.09	1.96	1.88	1.78	1.70	1.72	1.56	1.32	1.17

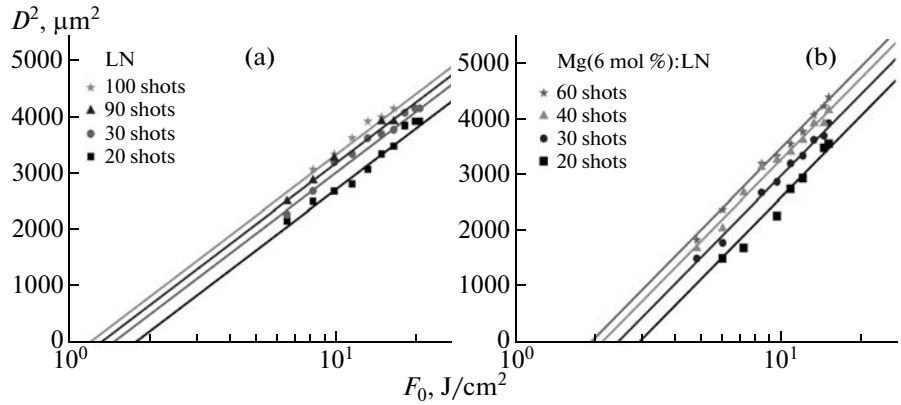

Fig. 5. Fitting results of squared diameter of ablated area versus laser fluence for (a) congruent LN and (b) Mg:LN.

same work was done to Mg-doped sample and presented in Fig. 4b.

Equation (3) was reused to gain the multi-shot ablation threshold fluence of the two materials. Taking the errors of measurements into consideration, the errors of the fitted line using the same slope as that of single shot is acceptable. Figure 5 demonstrates some fitting results. As was done to the single-shot situation, the ablation threshold fluence of the two samples under different number of shots was arranged in table.

It is obvious that the threshold fluence is affected by the number of shots impinging on the sample surface. For both the LN and Mg:LN samples, the threshold declines incisively when the shot number is relatively small and veers from each other gently when they undergo more shots, also reported by other groups [19, 20]. That can be explained by the incubation effect which appears as a result of the accumulation of laser-induced material defects and finally leads to surface damage, discussed in several previous studies [20–23]. As mentioned in these papers, the laser shot number dependency of the surface damage threshold of N shots $F_{th}(N)$ can be described in the following direct way:

$$F_{th}(N) = F_{th}(\infty) + [F_{th}(1) - F_{th}(\infty)] \times \exp[-k(N-1)], \quad (4)$$

where $F_{th}(\infty)$ is the minimum irradiated threshold fluence required infinite number of pulses to initiate the defect accumulation and $F_{th}(1)$ refers to the single-shot threshold. The strength of defect accumulation and the increase in photon absorption are characterized by an empirical parameter k [23]. The best fit of Eq. (4) of the data in table is exhibited in Fig. 6 for the both crystals as the laser wavelength is 800 nm and its pulse duration equals to 80 fs. It can be seen clearly in Fig. 6 that the surface-ablation threshold trends to be a constant as the pulse number mounts up. The threshold fluence for an infinite number of pulses $F_{th}(\infty)$ converges to a constant of 1.17 ± 0.02 J/cm^2 with the incubation parameter $k = 0.08$ to the lithium niobate sample, and stabilizes at 1.48 ± 0.08 J/cm^2 at $k = 0.046$ to the 6 mol % Mg-doped one.

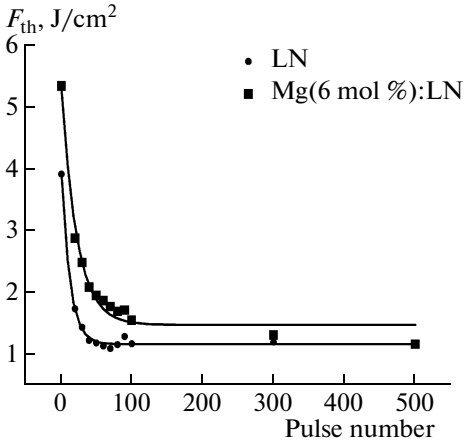

Fig. 6. Fit of threshold fluence as a function of the number of pluses by Eq. (4) for both LN and Mg:LN at $\lambda = 800$ nm and $\tau = 80$ fs.

In accumulation effect model, a small fraction of Frenkel pairs formed by multi-photon ionization may not combine and finally shape into color centers [24, 25]. With the increase of laser pulse, the absorption center enlarges in succession and eventually brings about the macro damage. There is also the possibility that the formation of color centers by direct trapping of conduction band electrons without the necessity of forming self-trapped excitons in advance [23]. Due to the great reduction of trapping cross section for electrons after heavy doping of Mg [26], it is harder to generate color center, which is manifested by the smaller incubation parameter and a slower trend to convergence for 6 mol % Mg-doped lithium niobate, as a symbol of weaker accumulation effect. Meanwhile, the difference of the laser fluence under infinite laser shots between the two crystals agrees with the study of

higher optical damage resistance of lithium niobate crystal doped with Mg [27] and our discussion in single-shot section.

CONCLUSION

The femtosecond laser surface ablation experiments of congruent and 6 mol % Mg-doped lithium niobate were conducted by single pulse and multi pluses. The ablation thresholds are 3.92 J/cm^2 for congruent lithium niobate and 5.34 J/cm^2 for Mg-doped lithium niobate under single shot. Band gap broadening after doping makes the lager single-shot ablation threshold for Mg-doped lithium niobate. It is also verified by the multi-shot experimental results, merely accumulation effect should be taken into consideration for more. Shot-number dependence on the modification threshold fluence indicates a convergence of the threshold to 1.17 ± 0.02 J/cm^2 for the lithium niobate sample and 1.48 ± 0.08 J/cm^2 for the 6 mol % Mg-doped one. The large reduction of trapping cross section for electrons after doping of Mg is account for the weaker incubation effect of doped lithium niobate.

ACKNOWLEDGMENTS

This research was supported by the National Natural Science Foundation of China (no. 10734080 and no. 10574092); the National Basic Research Program "973" of China (no. 2006CB806000), and the Shanghai Leading Academic Discipline Project (B201).

REFERENCES

1. R. P. Thomson, S. Campbell, I. J. Blewett, A. K. Kar, and D. T. Reid, Appl. Phys. Lett. **88**, 111109 (2006).
2. H. Chen, X. Chen, Y. Zhang, and Y. Xia, Laser Phys. **17**, 1378 (2007).
3. G. Zhou and M. Gu, Appl. Phys. Lett. **87**, 241107 (2005).
4. A. Askin, G. D. Boyd, J. M. Dziedzic, R. G. Smith, A. A. Ballman, J. J. Levinstein, and K. Nassau, Appl. Phys. Lett. **9**, 72 (1966).
5. D. A. Bryan, R. Gerson, and H. E. Tomaschke, Appl. Phys. Lett. **44**, 847 (1984).
6. A. M. Glass, Science **222**, 657 (1984).
7. A. A. Savchenkov, A. B. Matsko, D. Strekalov, V. S. Ilchenko, and L. Maleki, Appl. Phys. Lett. **88**, 241909 (2006).
8. T. Volk, N. Rubinina, and M. Wöhlecke, J. Opt. Soc. Am. B: Opt. Phys. **11**, 1681 (1994).
9. R. F. Z. Lizarelli, M. M. Costa, E. Carvalho-Filho, F. D. Nunes, and V. S. Bagnato, Laser Phys. Lett. **5**, 63 (2008).
10. I. V. Shutov, V. A. Enikeeva, I. A. Ozheredov, A. P Shkurinov, A. V. Shumitsky, and D. B. Yusupov, in *Proc. of the ICONO 2007 Conf., Minsk, Belarus*, Proc. of SPIE **6729**, 7292 (2007).
11. Z. Zheng, A. M. Weiner, K. R. Parameswaran, M. H. Chou, and M. M. Fejer, in *Proc. of the Conf. on Lasers and Electro-Optics, Baltimore, MD, USA*, Technical Digest, IEEE Cat. No. 01CH37170 (2001), p. 547.
12. T. Andres, R. Haag, S. Reuter, S. Zelt, J. P. Meyn, A. Borsutzky, R. Beigang, and R. Wallenstein, in *Proc. of the Conf. on Lasers and Electro-Optics, Long Beach, CA, USA*, Technical Digest, IEEE Cat. No. 02CH37337 (2002), p. 258.
13. J. Zhang, Y. Chen, F. Lu, and X. Chen, Opt. Express **16**, 6957 (2008).
14. J. Bonse, J. M. Wrobel, J. Krüger, and W. Kautek, Appl. Phys. A **72**, 89 (2001).
15. D. C. Deshpande, A. P. Malshe, E. A. Stach, V. Radmilovic, D. Alexander, D. Doerr, and D. Hirt, J. Appl. Phys. **97**, 074316 (2005).
16. L. V. Keldysh, Sov. Phys. JETP **20**, 1307 (1965).
17. B. H. Christensen and P. Balling, Phys. Rev. B: Condens. Matter **75**, 155424 (2009).
18. J. J. Xu, G. Y. Zhang, F. F. Li, X. Z. Zhang, Q. Sun, S. M. Liu, F. Song, Y. F. Kong, X. J. Chen, H. J. Qiao, J. H. Yao, and L. J. Zhao, Opt. Lett. **25**, 129 (2000).
19. A. Rodenas, Garcia J. A. Sanz Garcia, D. Jaque, G. A. Torchia, C. Mendez, I. Arias, L. Roso, and F. Agullo-Rueda, J. Appl. Phys. **100**, 033521 (2006).
20. K. Jamshidi-Ghaleh, D. Abdolahpour, and N. Mansour, Laser Phys. Lett. **3**, 573 (2006).
21. A. B. Yakar and R. L. Byer, J. Appl. Phys. **96**, 5316 (2004).
22. X. C. Wang, G. C. Lim, H. Y. Zheng, F. L. Ng, W. Liu, and S. J. Chua, Appl. Surf. Sci. **228**, 221 (2004).
23. D. Ashkenasi, M. Lorenz, R. Stoian, and A. Rosenfeld, Appl. Surf. Sci. **150**, 101 (1999).
24. R. T. Williams, Opt. Eng. **28**, 1024 (1989).
25. N. Itoh and K. Tanimura, Opt. Eng. **28**, 1034 (1989).
26. R. Gerson, J. F. Kirchhoff, L. E. Halliburton, and D. A. Bryan, J. Appl. Phys. **60**, 3553 (1086).
27. L. Pálfalvi, J. Hebling, G. Almási, Á. Péter, K. Polgár, K. Lengyel, and R. Szipücs, J. Appl. Phys. **95**, 902 (2004).